



Published in final edited form as:

Calcif Tissue Int. 2008 June ; 82(6): 489–497. doi:10.1007/s00223-008-9142-5.

Mechanical Stimulation of Bone Formation is Normal in the SAMP6 Mouse

Matthew J. Silva and Michael D. Brodt

Abstract

With aging the skeleton may have diminished responsiveness to mechanical stimulation. The senescence accelerated mouse SAMP6 has many features of senile osteoporosis and is thus a useful model to examine how the osteoporotic skeleton responds to mechanical loading. We performed in vivo tibial bending on four-month old SAMP6 (osteoporotic) and SAMR1 (control) mice. Loading was applied daily (60 cycles/day, 5 days/wk) for 2 weeks at peak force levels that produced estimated endocortical strains of 1000 and 2000 $\mu\epsilon$. In a separate group of mice, sham bending was applied. Comparisons were made between right (loaded) and left (non-loaded) tibiae. Tibial bone marrow cells were cultured under osteogenic conditions, and stained for alkaline phosphatase (ALP) and alizarin red (ALIZ) at 14 and 28 days, respectively. Tibiae were then embedded in plastic, sectioned and endocortical bone formation was assessed based on calcein labels. Tibial bending did not alter the osteogenic potential of the marrow as there were no significant differences in ALP or ALIZ staining between loaded and non-loaded bones. Tibial bending activated the formation of endocortical bone in both SAMP6 and SAMR1 mice, whereas sham bending did not elicit an endocortical response. Both groups of mice exhibited bending strain-dependent increases in bone formation rate. We found little evidence of diminished responsiveness to loading in the SAMP6 skeleton. In conclusion, the ability of the SAMP6 mouse to respond normally to an anabolic mechanical stimulus distinguishes it from chronologically aged animals. This finding highlights a limitation of the SAMP6 mouse as a model of senile osteoporosis.

Introduction

Senile osteoporosis is attributed to diminished bone formation with aging [1,2]. Reductions in histological measures of bone formation in aged and/or osteoporotic individuals [3–7] are consistent with decreased osteoblast numbers. Adult osteoblasts likely originate from bone marrow osteoprogenitors [8,9], and a number of studies support the concept that the osteogenic potential of bone marrow is reduced with aging [8,10–16]. Thus, fewer marrow osteoprogenitors or a reduced ability of progenitors to differentiate may contribute to reduced endosteal bone formation in senile osteoporosis.

Mechanical loading is a potent stimulus of bone formation. However, several animal studies indicate that with aging the skeleton is less responsive to mechanical loading. Ulnar compression in aged turkeys [17], and tibial bending in aged rats [18] and mice [19] have each demonstrated a lower level of responsiveness than when the same level of stimulus was applied

Correspondence to: Matthew J. Silva, Ph.D., Department of Orthopaedic Surgery, Washington University School of Medicine, 1 Barnes-Jewish Hospital Plaza, Suite 11300 WP, St. Louis, Missouri 63110, email: E-mail: silvam@wustl.edu, Telephone: (314) 362-8585, FAX: (314) 362-0334.

Presented in part at the 2004 meeting of the American Society of Bone and Mineral Research, and the 2005 meeting of the Orthopaedic Research Society

The original publication is available at www.springerlink.com.

to younger animals. It is unclear if these effects are related to fewer osteoblasts and/or diminished basal rates of bone formation with aging. One *in vitro* study reported no loss of mechanosensitivity in human bone cells [20], supporting the notion that reduced osteoblast number rather than reduced osteoblast vigor [21] explains the apparent age-related decline in mechanoresponsiveness.

The senescence accelerated mouse SAMP6 has many features of senile osteoporosis, including diminished rates of endosteal bone formation, fewer marrow osteoprogenitors and reduced bone strength compared to age-matched SAMR1 controls [22–26]. SAMP6 mice are therefore a useful model to examine the issue of whether or not the osteoporotic skeleton is less responsive to mechanical loading.

Our objective was to examine the skeletal mechanoresponsiveness of the SAMP6 mouse. We performed *in vivo* tibial bending in SAMP6 (osteoporotic) and SAMR1 (control) mice and assessed changes in bone formation and marrow osteogenic potential. Because of its early aging phenotype, we hypothesized that SAMP6 mice have a diminished response to mechanical loading.

Methods

Animals

A total of 57 male mice (32 SAMR1, 25 SAMP6) were obtained at 4–5 mos. age from our breeding colony following approval by our institutional Animal Studies Committee. SAMR1 and SAMP6 mice were maintained as separate inbred strains from breeders originally provided by the Council for SAM Research (Kyoto University, Japan). SAMR1 is one of the SAM 'Resistant' strains and is considered an appropriate control for SAMP6 [23]. The osteoporotic phenotype is evident by 4 months age in SAMP6 mice [22–24]. Mice were housed up to five per cage, with 12:12 hour light:dark cycles and access to standard mouse chow and water *ad libitum*.

In Vivo Loading – Tibial Bending

The right tibiae of 43 mice (22 SAMR1, 21 SAMP6) were loaded in three-point bending using a modified version of the method described by Akhter et al.[27]. Left tibiae were not loaded and served as contralateral controls. We selected the tibia due to its large marrow cavity, and we focused on the endocortical surface rather than the periosteal surface because of our interest in marrow-bone interactions. For loading, the right lower hindlimb was placed in a bending fixture attached to a servohydraulic materials testing machine (Instron 8841). In this fixture, application of a transverse force at the mid-diaphysis produces tibial bending (Fig. 1A).

Mice were assigned at random to one of two loading groups based on the level of mechanical strain ($n = 10\text{--}11/\text{group}$ for each SAMR1 and SAMP6). Values of applied force were chosen to produce a peak endocortical strain of either 1000 or 2000 microstrain ($\mu\epsilon$) (Table 1). Because endocortical strains cannot be measured directly, we estimated their values using periosteal strain data and engineering analysis, as described in detail previously [28]. Forces for the SAMP6 group were ~20% greater than for SAMR1 due to the greater moment of inertia of the SAMP6 tibia. (A third force level corresponding to 3000 $\mu\epsilon$ was included at the beginning of this study, but three of three mice from this group developed lameness in the right hindlimb during the second week of loading and we discontinued this group.)

Loading was conducted on days 1–5 and 8–12 of a 15-day protocol [29]. Mice were anesthetized (1–3% inhaled isoflurane) and positioned in the loading fixture. A 1 N compressive preload was applied, followed by 60 cycles of rest-inserted loading [19] (triangle waveform to the target peak force at 80 N/s load and unload, followed by a 10 s rest interval).

After loading mice were returned to their cages and allowed unrestricted activities. Calcein (7 mg/kg; Sigma) was administered by i.p. injection on days 5 and 12 to label bone forming surfaces. Mice were killed on day 15 by CO₂ asphyxiation.

In Vivo Loading – Sham Tibial Bending

A second cohort of 14 mice (10 SAMR1, 4 SAMP6) were loaded using a sham bending protocol to determine if periosteal compression by itself elicited an endocortical response. Rather than apply three-point bending, we applied two-point transverse compression, with a single support point directly opposite the loading point at the tibial midshaft (Fig. 1B). When the loading point displaced downward, local compression was generated at the medial and lateral tibial surfaces, but no net bending. Peak force values and all other aspects of the loading protocol were identical to the tibial bending experiment.

Bone Marrow Cell Culture

To determine if the relative osteogenic potential of the marrow was altered by tibial bending, we cultured adherent bone marrow stromal cells as described [25]. Briefly, bilateral tibiae were dissected immediately post mortem and bone marrow flushed using standard culture medium (α -minimum essential medium [Mediatech cellgro, MT10022CV, Fisher], with 10% heat inactivated fetal bovine serum [FBS; SH30071.03; Hyclone Laboratories] and penicillin/streptomycin [Washington Univ. Tissue Culture Support Center]). The FBS was from a single manufacturer's lot. The marrow was then filtered (70 μ m) and centrifuged (1150 RPM, 10 minutes, 4°C), and the cells were resuspended in fresh medium. The cells were plated on 12-well plastic culture plates at 3.6×10^6 cells/well in 2 ml of medium. There were 4–8 replicate wells per tibia, divided between two plates. Cells from paired (left, right) tibiae were plated in adjacent rows on the same plates. Plates were kept in a humidified incubator (5% CO₂, 37°C). On day 3, non-adherent cells were discarded and the medium changed to one that supports osteoblast differentiation (standard media plus 13 mM β glycerophosphate [G-9891, Sigma] and 50 mg/L L-ascorbic acid [A-4544, Sigma]). This osteogenic medium was used throughout the rest of the culture period, with complete changes twice per week.

On day 14, half of the plates were stained for the alkaline phosphatase (ALP) enzyme using a commercial kit (85-L; Sigma) as per manufacturer's instructions. Positively stained fibroblastic colonies (CFU-F/ALP⁺) are considered to represent osteoprogenitors [13,30]. On day 28, mineral deposits on the remaining plates were stained with 2% alizarin red (A5533; Sigma). Positively stained colonies (CFU-OB) are taken to represent osteoblast colonies that deposited matrix that was then mineralized [23,31].

Digital images of each well were captured (1360×1024, Olympus DC70) under standardized lighting and camera settings. The images were loaded into an analysis program (Scion Image) as grayscale images (0–255 arbitrary density). Threshold values (105 for ALP, 65 for alizarin red) separating positive cells from background were chosen based on a sensitivity analysis. Percent positive area ($100 \times$ positive area/total well area) was computed. Values from replicate wells were averaged to get a single value of each parameter for each bone. The percent positive area is taken as an in vitro index of the osteogenic potential of the bone marrow. The effect of loading was analyzed using paired t-tests (right, loaded vs. left, control) and repeated measures analysis of variance (ANOVA) with mouse strain (SAMR1, SAMP6) and mechanical strain (1000, 2000 μ ϵ) as factors.

Histomorphometry

Immediately after bone marrow was flushed, tibiae were placed in 70% ethanol for 1 day. They were then dehydrated in ascending concentrations of ethanol (70–100%) and embedded in methylmethacrylate (Fisher) using standard procedures for undecalcified bone. Three

consecutive transverse sections (100 μ m thickness) were cut from the mid-shaft of each tibia, ~5 mm proximal from the distal tibiofibular junction (corresponding to the site of maximum bending strain[28]) using a saw microtome (Leica SP 1600). Sections were mounted on glass slides and viewed under UV excitation on a fluorescence equipped microscope (Leitz Orthoplan). Dynamic measures of endocortical bone formation were determined based on calcein labels using commercial software (Osteomeasure, Osteometrics). We determined percent single-(sLS/BS) and double-labeled (dLS/BS) bone surface, mineralizing surface (MS/BS), mineral apposition rate (MAR) and bone formation rate (BFR/BS) based on histomorphometry standards [32]. For samples with no detectable double label, MAR and BFR/BS were considered as missing data [33]. The periosteal surface was not analyzed quantitatively. The effect of loading was analyzed using paired t-tests (right, loaded vs. left, control) and repeated measures ANOVA with mouse strain (SAMR1, SAMP6) and mechanical strain (1000, 2000 μ ϵ) as factors.

Results

Both SAMR1 (control) and SAMP6 (osteoporotic) mice had increased measures of endocortical bone formation in response to two weeks of daily tibial bending. Mineralizing surface was increased significantly in loaded (right) vs. non-loaded (left) tibiae from SAMR1 and SAMP6 mice in both 1000 and 2000 μ ϵ loading groups, due primarily to significant increases in double-labeled bone surface ($p < 0.05$; Table 2). Double calcein labels were observed in 30 of 43 loaded tibiae but only four of 43 non-loaded tibiae (Fig. 2). Loaded tibiae from both SAMR1 and SAMP6 mice exhibited strain-dependent increases in mineral apposition rate and bone formation rate ($p < 0.05$ based on two-way ANOVA) (Fig. 3). The only evidence for a diminished responsiveness to loading in SAMP6 mice was that they did not exhibit a strain-dependent increase in double-labeled surface or mineralizing surface, whereas loaded tibiae from SAMR1 mice did ($p < 0.01$). Importantly, there were no significant differences (based on two-way ANOVA) in measures of bone formation between SAMR1 and SAMP6 mice, either when comparing absolute (loaded tibia) or relative (loaded tibia minus non-loaded tibia) data. At the periosteal surface, we observed woven bone formation on 16 of 22 tibiae from SAMR1 and 20 of 21 loaded tibiae from SAMP6. Woven bone was typically located on the lateral surface, corresponding to the site where the loading pad contacted the leg. There was no incidence of woven bone on the non-loaded controls. Qualitatively, the amount of woven bone was marginally greater for SAMP6 mice than SAMR1, consistent with their marginally elevated baseline rate of periosteal bone formation [25]. Lastly, there was no notable intracortical response to loading.

Sham tibial bending was performed to assess the effect of periosteal compression (without bending) on endocortical bone formation. Double-labeled bone surface was observed on only two of 14 loaded tibiae (and one of 14 non-loaded tibiae) (Fig. 4; Table 3). Paired comparisons between loaded versus non-loaded tibiae revealed no significant differences in single-labeled surface, double-labeled surface or mineralizing surface. Therefore, we found no evidence of increased endocortical bone formation due to periosteal compression. We did observe periosteal woven bone on sham-loaded tibiae, although the amount of woven bone was typically less than for three-point bending.

Tibial bending did not change the *in vitro* osteogenic potential of the bone marrow. Alkaline phosphatase staining after 14 days of bone marrow cell culture revealed no differences between loaded and non-loaded tibiae ($p = 0.53$, repeated measures ANOVA; Table 4). Similarly, alizarin red staining of mineralized nodules did not differ between loaded and control tibiae ($p = 0.14$). In addition, there were no differences between loading groups (1000 vs. 2000 μ ϵ). Alizarin red staining was greater in SAMP6 mice than in SAMR1 ($p = 0.011$), whereas alkaline phosphatase staining did not differ between mouse strains ($p = 0.97$).

Discussion

Our objective was to assess the skeletal mechanoresponsiveness of the SAMP6 mouse, a murine model of senile osteoporosis. Endocortical bone formation was activated by two weeks of daily tibial bending in 4-month old SAMP6 mice, similarly to age-matched SAMR1 controls. Both groups of mice exhibited bending strain-dependent increases in bone formation rate, i.e., a dose-response. The only indication of an impaired response in SAMP6 mice is that, in contrast to SAMR1, they did not demonstrate a dose-response increase in mineralizing surface. However, SAMP6 mice did demonstrate a dose-response increase in endocortical mineral apposition and bone formation rates. Taken together our data reveal little evidence of diminished responsiveness to loading in the SAMP6 skeleton. In addition, tibial bending did not alter the *in vitro* osteogenic potential of the bone marrow in either SAMP6 or SAMR1 mice.

There have been several reports on the responsiveness of the aged skeleton to mechanical loading. Studies that used direct (non-physiological) loading methods have indicated reduced responsiveness in aged versus young animals. The ulna of aged (3 yr.) turkeys was unresponsive to compressive loading at strain magnitudes that elicited robust periosteal and endocortical bone formation in younger (1 yr.) turkeys [17]. This failure to activate surface modeling in aged turkeys was in contrast to normal measures of bone formation associated with intracortical remodeling, indicating that the aged animals had the potential to form bone but required a greater stimulus. Similarly, tibiae from aged (19 mo.) rats had markedly lower rates of endocortical bone formation after two weeks of daily bending compared to tibiae from young adult (9 mo.) rats loaded to comparable levels of strain [18,34]. The strain threshold for activation of endocortical bone formation was much greater in the older rats, consistent with the concept that a greater loading stimulus is required with aging. In addition, tibiae from aged (22 mo.) C57Bl/6 mice were responsive to rest-inserted loading, but formed bone at approximately 40% of the rate of younger (4 mo.) mice [19]. Therefore, our finding that SAMP6 mice had no little or no deficit in mechanoresponsiveness compared to SAMR1 control mice indicates that the SAMP6 model of senile osteoporosis does not reflect the loss of mechanoresponsiveness reported with actual skeletal aging. This result, taken together with our previous finding that SAMP6 bones have a matrix flaw that does not mimic aging [26], calls into question the relevance of the SAMP6 mouse as a model of age-related osteoporosis.

The molecular basis for the low bone formation osteoporosis in SAMP6 mice is not clear. Recently, a possible role for secreted frizzled-related protein (Sfrp4) as a negative regulator of peak bone mass in SAMP6 mice has been described [35]. Sfrp4 expression is relatively high in SAMP6 bone, which might lead to inhibition of Wnt signaling and osteoblast proliferation [35]. Examination of changes in Wnt signaling due to loading in SAMP6 mice was beyond the scope of the current study, but our results suggest that any baseline defects related to Wnt signaling in SAMP6 mice can be overcome by mechanical stimulation. In addition, diminished osteoblastogenesis in SAMP6 mice has been linked to reduced interleukin (IL)-11 expression in bone marrow stromal cells [36,37]. Interestingly, parathyroid hormone (PTH) stimulates IL-11 expression in osteoblasts and bone marrow stromal cells [38,39], and PTH treatment increases bone formation rates in SAMP6 mice [40]. Moreover, mechanical stimulation of bone formation is PTH-dependent [41]. Thus, we hypothesize that the ability of SAMP6 mice to respond to mechanical loading reflects, more generally, an intact PTH response. Additional studies would be required to address this hypothesis and to determine if diminished mechanoresponsiveness with aging is linked to PTH.

Previous reports of skeletal unloading have indicated that the osteogenic potential of the bone marrow is diminished by *unloading*. Bone marrow cell cultures initiated 11 days after sciatic neurectomy had reduced alkaline phosphatase activity and mineralized nodule formation vs.

control [42]. Similarly, bone marrow cell cultures started 2–7 days after tail suspension unloading showed reduced cell proliferation, alkaline phosphatase activity and mineralized nodule formation as well as diminished responsiveness to PTH stimulation [43,44]. We are unaware of prior studies that have looked at changes in bone marrow cells after skeletal *overloading*. Our results indicate that 2 weeks of daily tibial bending does not increase the number of alkaline phosphatase positive or mineralized CFUs, suggesting that the osteogenic potential of the marrow, while sensitive to unloading, is not enhanced by increased loading. This finding is consistent with the view that in the short-term, loading acts to activate existing lining cells or committed osteoprogenitors [45,46] rather than alter lineage allocation. This in turn suggests that deficits in the bone marrow osteoprogenitor pool may not be responsible for any age-related changes in bone mechanoresponsiveness. Additional studies looking at marrow responses with other techniques (e.g., microarrays, stem cell deficient mice) are needed to provide more insight into the role, if any, of marrow stem cells in supporting loading-induced bone formation.

There are several limitations to our study. First, we relied on estimated values of endocortical strain to equate the mechanical stimuli at the endocortical surfaces of SAMR1 and SAMP6 mice. It is not possible to directly measure endocortical strains, so we relied on periosteal data combined with finite element analysis to estimate the endocortical strains in our loading model [28]. It is possible that errors in these estimates may have led to differences in the level of stimuli applied to the different mouse strains. A second limitation is that the tibial bending method we used generates direct periosteal pressure at the points of contact, which likely contributes to the periosteal woven bone response at the site of interest. For this reason, and also because of our interest in bone-marrow interactions, we focused on the endocortical response. Importantly, the sham tibial bending case (Fig. 1B) did not elicit an endocortical response (Fig. 4). A null response at the endocortex following sham bending has been noted by others in mice [47] and rats [34]. Thus, we do not believe that periosteal contact directly contributed to the endocortical response we observed. Nonetheless, it is clear that high bending strains plus periosteal contact led to robust periosteal woven bone formation in the majority of loaded tibiae (Fig. 2). It is not possible using non-invasive means to generate endocortical strains great enough to activate endocortical bone formation without also generating even larger periosteal strains, which will in turn stimulate a periosteal response. Thus, in our loading model and others, the bone may act as an organ, and it is possible that responses on the periosteal surface influence endocortical responses. Nonetheless, this should not affect our main study objective which was to compare SAMP6 and SAMR1 mice exposed to similar stimuli. Notably, we recently used the same loading method and found significant differences in endocortical bone formation between wildtype and connexin 43-null mice, even though both genotypes had exuberant periosteal woven bone formation [29].

Another limitation of our study is that measures of bone formation and marrow CFUs from non-loaded limbs of SAMP6 mice were, unexpectedly, not less than non-loaded limbs from SAMR1 controls. This finding contradicts previous reports by us and others of diminished endosteal bone formation and marrow osteogenic indices in age-matched SAMP6 mice vs. SAMR1 [22,23,25]. It is possible that the SAMP6 mice in the current study had a systemic response to the loading protocol and/or anesthesia that upregulated their basal skeletal metabolism. This in turn may have made them better able to respond to skeletal loading. Thus, our conclusion that loading was able to activate localized bone formation equally well in SAMP6 and SAMR1 mice carries the caveat that a systemic response may have contributed to the local response.

In summary, two weeks of daily tibial bending activated endocortical bone formation in SAMP6 and SAMR1 mice but did not enhance the osteogenic potential of the bone marrow. Both strains of mice exhibited dose-response increases in bone formation, and overall there

was little evidence of diminished responsiveness to loading in SAMP6 mice. Whatever the mechanism is for the low bone formation phenotype of SAMP6 mice, mechanical loading is able to overcome it. This finding is consistent with the ability of other anabolic stimuli such as PTH to stimulate bone formation in SAMP6 mice [40]. In conclusion, the ability of the SAMP6 mouse to respond normally to an anabolic mechanical stimulus distinguishes it from chronologically aged animals [17–19], indicating an important limitation of the SAMP6 model as a model of senile osteoporosis.

Acknowledgments

The authors thank Mike Ko for performing the cell culture assays. This study was funded by a grant from the National Institutes of Health (NIAMS AR47867). Animals were housed in a facility supported by an NIH grant (NCRR C06 RR015502).

References

1. Riggs BL, Melton LJ. Evidence for two distinct syndromes of involutonal osteoporosis. *Am J of Med* 1983;75:899–901. [PubMed: 6650542]
2. Kassem, M.; Melton, L.J.; Riggs, B.L. The type I/type II model for involutonal osteoporosis. In: Marcus, R.; Feldman, D.; Kelsey, J., editors. *Osteoporosis*. Academic Press; San Diego: 1996. p. 691-702.
3. Lips P, Courpron P, Meunier PJ. Mean wall thickness of trabecular bone packets in the human iliac crest: changes with age. *Calcif Tiss Res* 1978;26:13–17.
4. Darby AJ, Meunier PJ. Mean wall thickness and formation periods of trabecular bone packets in idiopathic osteoporosis. *Calcified Tissue International* 1981;33:199–204. [PubMed: 6791782]
5. Parfitt AM, Villanueva AR, Foldes J, Rao DS. Relations between histologic indices of bone formation: implications for the pathogenesis of spinal osteoporosis. *J Bone Miner Res* 1995;10:466–473. [PubMed: 7785469]
6. Recker RR, Kimmel DB, Parfitt AM, Davies KM, Keshawarz N, Hinders S. Static and tetracycline-based bone histomorphometric data from 34 normal postmenopausal females. *J Bone Miner Res* 1988;3:133–144. [PubMed: 3213608]
7. Clarke BL, Ebeling PR, Jones JD, Wahner HW, O'Fallon WM, Riggs BL, Fitzpatrick LA. Changes in quantitative bone histomorphometry in aging healthy men. *Journal of Clinical Endocrinology & Metabolism* 1996;81:2264–2270. [PubMed: 8964862]
8. Friedenstein AJ. Precursor cells of mechanocytes. *Int Rev Cytol* 1976;47:327–359. [PubMed: 11195]
9. Beresford JN. Osteogenic stem cells and the stromal system of bone and marrow. *Clin Ortho Rel Res* 1989;240:270–280.
10. Gimble JM, Robinson CE, Wu X, Kelly KA. The function of adipocytes in the bone marrow stroma: an update. *Bone* 1996;19:421–428. [PubMed: 8922639]
11. Bergman RJ, Gazit D, Kahn AJ, Gruber H, McDougall S, Hahn TJ. Age-related changes in osteogenic stem cells in mice. *J Bone Miner Res* 1996;11:568–577. [PubMed: 9157771]
12. Kahn A, Gibbons R, Perkins S, Gazit D. Age-related bone loss: a hypothesis and initial assessment in mice. *Clin Ortho Rel Res* 1995;313:69–75.
13. D'ippolito G, Schiller PC, Ricordi C, Roos BA, Howard GA. Age-related osteogenic potential of mesenchymal stromal stem cells from human vertebral bone marrow. *J Bone Miner Res* 1999;14:1115–1122. [PubMed: 10404011]
14. Mueller SM, Glowacki J. Age-related decline in the osteogenic potential of human bone marrow cells cultured in three-dimensional collagen sponges. *J Cell Biochem* 2001;82:583–590. [PubMed: 11500936]
15. Stenderup K, Justesen J, Clausen C, Kassem M. Aging is associated with decreased maximal life span and accelerated senescence of bone marrow stromal cells. *Bone* 2003;33:919–926. [PubMed: 14678851]
16. Sethe S, Scutt A, Stolzing A. Aging of mesenchymal stem cells. *Ageing Res Rev* 2006;5:91–116. [PubMed: 16310414]

17. Rubin CT, Bain SD, McCleod KJ. Suppression of osteogenic response in the aging skeleton. *Calcif Tiss Int* 1992;50:306–313.
18. Turner CH, Takano Y, Owan I. Aging changes mechanical loading thresholds for bone formation in rats. *J Bone Miner Res* 1995;10:1544–1549. [PubMed: 8686511]
19. Srinivasan S, Agans SC, King KA, Moy NY, Poliachik SL, Gross TS. Enabling bone formation in the aged skeleton via rest-inserted mechanical loading. *Bone* 2003;33:946–955. [PubMed: 14678854]
20. Klein-Nulend J, Sterck JGH, Semeins CM, Lips P, Joldersma M, Baart JA, Burger EH. Donor age and mechanosensitivity of human bone cells. *Osteoporosis Int* 2002;13:137–146.
21. Manolagas SC. Editorial: cell number versus cell vigor - what really matters to a regenerating skeleton? *Endocrinol* 1999;4377–4381.
22. Suda, T.; Miyama, K.; Uchiyama, Y.; Katagiri, T.; Yamaguchi, A.; Sato, T. Osteoporotic bone changes in SAMP6 are due to a decrease in osteoblast progenitor cells. In: Takeda, T., editor. *The SAM model of senescence: proceedings of the first intl conf on senescence, the SAM model*. Elsevier Science; Kyoto, Japan: 1994. p. 47-52.
23. Jilka RL, Weinstein RS, Takahashi K, Parfitt AM, Manolagas SC. Linkage of decreased bone mass with impaired osteoblastogenesis in a murine model of accelerated senescence. *J Clin Invest* 1996;97:1732–1740. [PubMed: 8601639]
24. Silva MJ, Brodt MB, Ettner SL. Long bones from the senescence accelerated mouse SAMP6 have increased size but reduced whole-bone strength and resistance to fracture. *J Bone Miner Res* 2002;17:1597–1603. [PubMed: 12211429]
25. Silva MJ, Brodt MD, Ko M, Abu-Amer Y. Impaired marrow osteogenesis is associated with reduced endocortical bone formation but does not impair periosteal bone formation in long bones of SAMP6 mice. *J Bone Miner Res* 2005;20:419–427. [PubMed: 15746986]
26. Silva MJ, Brodt MD, Wopenka B, Thomopoulos S, Williams D, Wassen MH, Ko M, Kusano N, Bank RA. Decreased Collagen Organization and Content Are Associated With Reduced Strength of Demineralized and Intact Bone in the SAMP6 Mouse. *J Bone Miner Res* 2006;21:78–88. [PubMed: 16355276]
27. Akhter MP, Cullen DM, Pedersen EA, Kimmel DB, Recker RR. Bone response to in vivo mechanical loading in two breeds of mice. *Calcif Tiss Int* 1998;63:442–449.
28. Silva MJ, Brodt MD, Hucker WJ. Finite element analysis of the mouse tibia: Estimating endocortical strain during three-point bending in SAMP6 osteoporotic mice. *Anat Rec A Discov Mol Cell Evol Biol* 2005;283A:380–390. [PubMed: 15747345]
29. Grimston SK, Brodt MD, Silva MJ, Civitelli R. Attenuated Response to in vivo Mechanical Loading in Mice with Conditional Osteoblast Ablation of the Connexin43 Gene (Gja1)*. *J Bone Miner Res*. 2008 Feb 18;[Epub ahead of print]
30. Dimai HP, Linkhart TA, Linkhart SG, Donahue LR, Beamer WG, Rosen CJ, Farley JR, Baylink DJ. Alkaline phosphatase levels and osteoprogenitor cell numbers suggest bone formation may contribute to peak bone density differences between two inbred strains of mice. *Bone* 1998;22:211–216. [PubMed: 9514213]
31. Aubin JE. Osteoprogenitor cell frequency in rat bone marrow stromal populations: role for heterotypic cell-cell interactions in osteoblast differentiation. *J Cell Biochem* 1999;72:396–410. [PubMed: 10022521]
32. Parfitt AM, Drezner MK, Glorieux FH, Kanis JA, Malluche H, Meunier PJ, Ott SM, Recker RR. Bone histomorphometry: standardization of nomenclature, symbols, and units. *J Bone Min Res* 1987;2:595–610.
33. Foldes J, Shih MS, Parfitt AM. Frequency distributions of tetracycline-based measurements: implications for the interpretation of bone formation indices in the absence of double-labeled surfaces. *J Bone Miner Res* 1990;5:1063–1067. [PubMed: 2080717]
34. Turner CH, Forwood MR, Rho JY, Yoshikawa T. Mechanical loading thresholds for lamellar and woven bone formation. *J Bone Min Res* 1994;9:87–97.
35. Nakanishi R, Shimizu M, Mori M, Akiyama H, Okudaira S, Otsuki B, Hashimoto M, Higuchi K, Hosokawa M, Tsuboyama T, Nakamura T. Secreted frizzled-related protein 4 is a negative regulator of peak BMD in SAMP6 mice. *J Bone Miner Res* 2006;21:1713–1721. [PubMed: 17002585]

36. Kodama Y, Takeuchi Y, Suzawa M, Fukumoto S, Murayama H, Yamato H, Fujita T, Kurokawa T, Matsumoto T. Reduced expression of interleukin-11 in bone marrow stromal cells of senescence-accelerated mice (SAMP6): relationship to osteopenia with enhanced adipogenesis. *J Bone Miner Res* 1998;13:1370–1377. [PubMed: 9738508]
37. Tohjima E, Inoue D, Yamamoto N, Kido S, Ito Y, Kato S, Takeuchi Y, Fukumoto S, Matsumoto T. Decreased AP-1 activity and interleukin-11 expression by bone marrow stromal cells may be associated with impaired bone formation in aged mice. *J Bone Miner Res* 2003;18:1461–1470. [PubMed: 12929935]
38. Elias JA, Tang W, Horowitz MC. Cytokine and hormonal stimulation of human osteosarcoma interleukin-11 production. *Endocrinology* 1995;136:489–498. [PubMed: 7835281]
39. Kim GS, Kim CH, Choi CS, Park JY, Lee KU. Involvement of different second messengers in parathyroid hormone- and interleukin-1-induced interleukin-6 and interleukin-11 production in human bone marrow stromal cells. *J Bone Miner Res* 1997;12:896–902. [PubMed: 9169347]
40. Clement-Lacroix P, Ai M, Morvan F, Roman-Roman S, Vayssiere B, Belleville C, Estrera K, Warman ML, Baron R, Rawadi G. Lrp5-independent activation of Wnt signaling by lithium chloride increases bone formation and bone mass in mice. *Proc Natl Acad Sci U S A* 2005;102:17406–17411. [PubMed: 16293698]
41. Chow JW, Fox S, Jagger CJ, Chambers TJ. Role for parathyroid hormone in mechanical responsiveness of rat bone. *Am J Physiol* 1998;274:E146–154. [PubMed: 9458760]
42. Keila S, Pitaru S, Grosskopf A, Weinreb M. Bone marrow from mechanically unloaded rat bones expresses reduced osteogenic capacity in vitro. *J Bone Miner Res* 1994;9:321–327. [PubMed: 8191925]
43. Kostenuik PJ, Halloran BP, Morey-Holton ER, Bikle DD. Skeletal unloading inhibits the in vitro proliferation and differentiation of rat osteoprogenitor cells. *Am J Physiol* 1997;273:E1133–E1139. [PubMed: 9435529]
44. Kostenuik PJ, Harris J, Halloran B, Turner RT, Morey-Holton ER, Bikle DD. Skeletal unloading causes resistance of osteoprogenitor cells to parathyroid hormone and to insulin-like growth factor-I. *J Bone Miner Res* 1999;14:21–31. [PubMed: 9893062]
45. Chow JW, Wilson AJ, Chambers TJ, Fox SW. Mechanical loading stimulates bone formation by reactivation of bone lining cells in 13-week-old rats. *J Bone Miner Res* 1998;13:1760–1767. [PubMed: 9797486]
46. Turner CH, Owan I, Alvey T, Hulman J, Hock JM. Recruitment and proliferative responses of osteoblasts after mechanical loading in vivo determined using sustained-release bromodeoxyuridine. *Bone* 1998;22:463–469. [PubMed: 9600779]
47. Akhter MP, Cullen DM, Recker RR. Bone adaptation response to sham and bending stimuli in mice. *J Clin Densitom* 2002;5:207–216. [PubMed: 12110765]

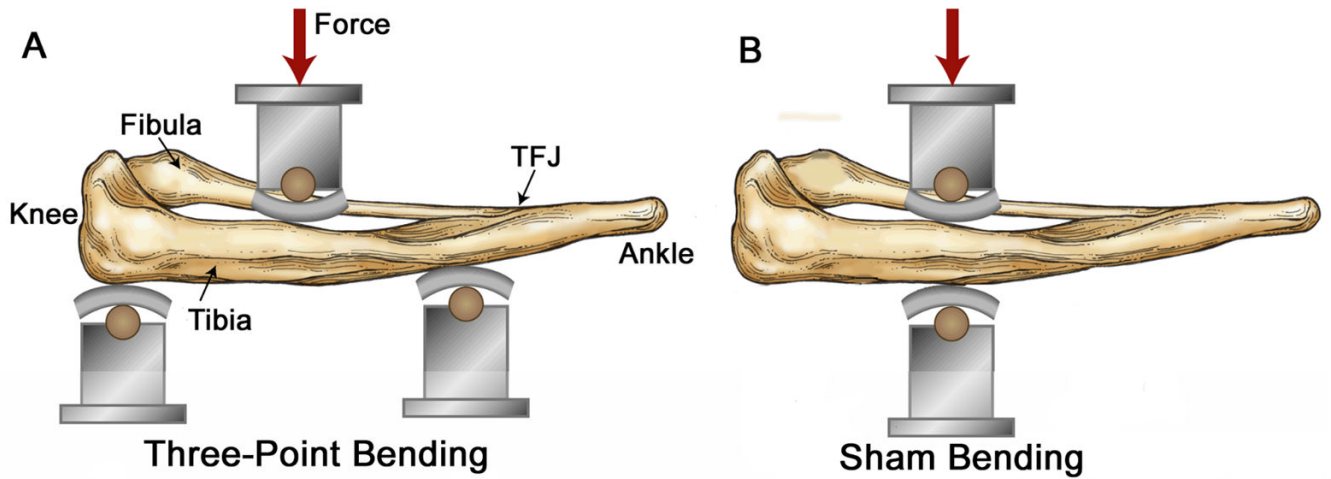


Figure 1.

Sketch showing skeletonized view of mouse lower hindlimb positioned for in vivo mechanical loading. (A) For three-point bending, the medial surface of the leg was positioned over two supports spaced 10 mm apart, with the proximal support contacting just distal to the knee joint and the distal support contacting near the distal tibiofibular junction (TFJ). The loading point contacted the lateral surface of the leg at the midpoint between the two supports. The contact points were 1.8 mm diameter wooden dowels covered with a 2-mm thick rubber pads. In this setup, downward movement of the loading point produces tibial bending in the medial-lateral plane with tension on the medial surface [28]. (B) For sham bending, a single support point is placed opposite the loading point so that application of force does not produce bending of the tibia. (Figure modified from [28]).

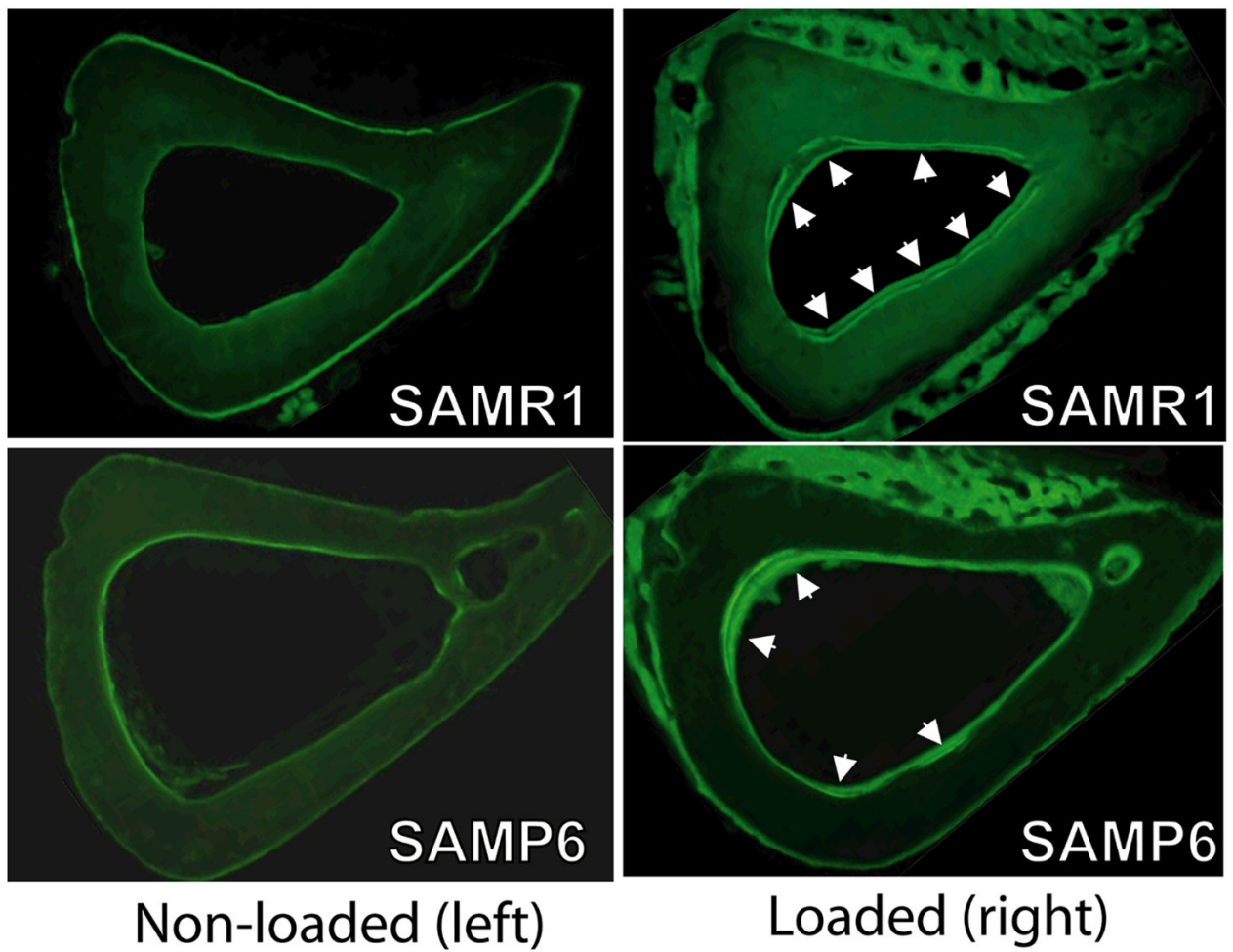


Figure 2. Fluorescent photomicrographs illustrating increased bone formation in SAMR1 and SAMP6 tibiae subjected to bending (right) versus non-loaded controls (left) (specimens shown are from 2000 $\mu\epsilon$ loading groups). In particular, loading increased the endocortical double-labeled surface (arrowheads). Histomorphometric analysis was performed on the endocortical surface only.

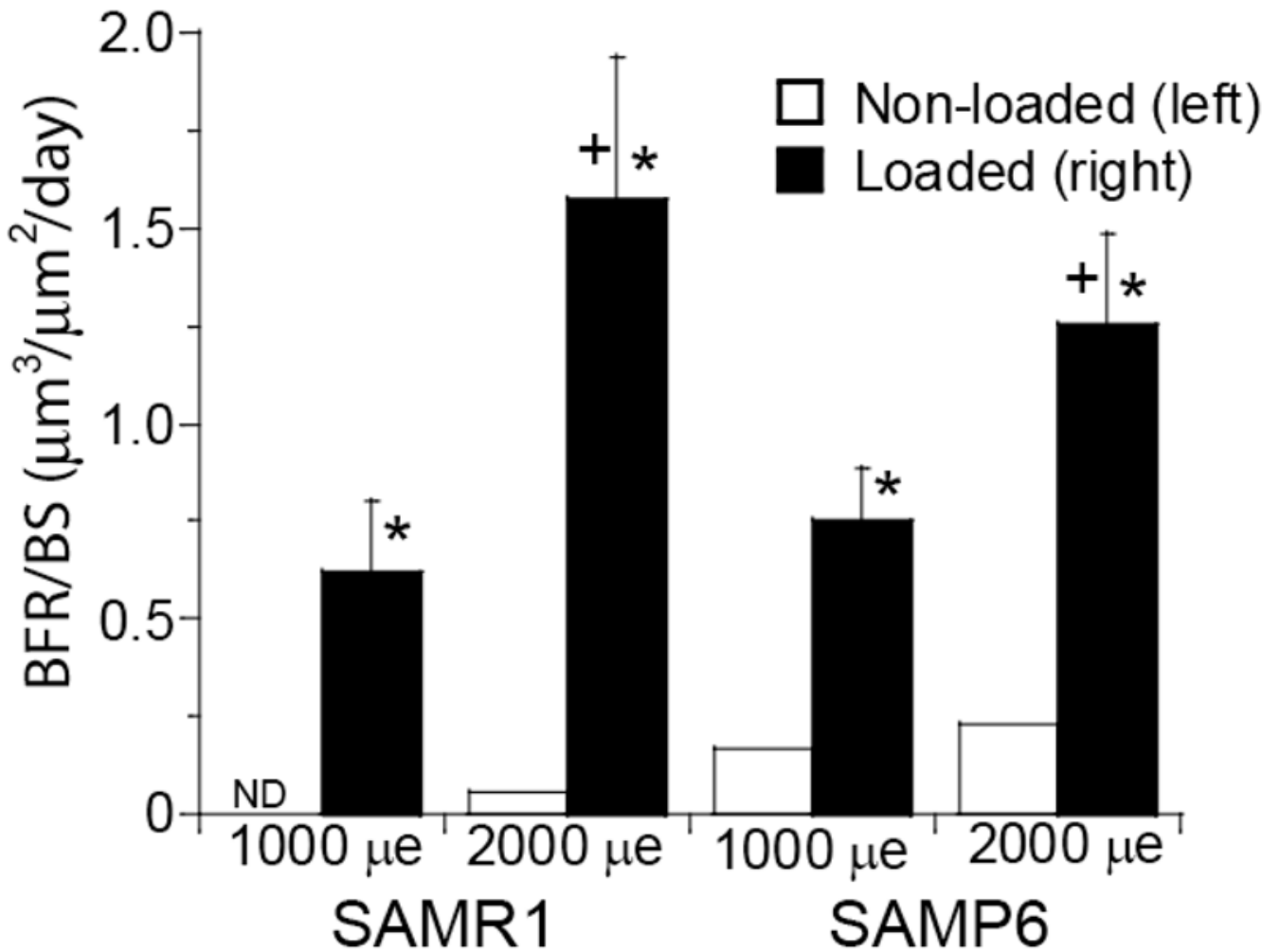


Figure 3.

Endocortical bone formation rate (mean \pm SE) was significantly increased in loaded tibiae of both SAMR1 and SAMP6 mice compared to zero and to average value of non-loaded tibia (* $p < 0.05$, unpaired t-test). Bone formation rate increased with increasing bending strain (2000 μe different from 1000 μe , $p = 0.011$ by two-way ANOVA; + $p < 0.07$ for individual comparisons within the same mouse strain). There were no significant difference between SAMR1 and SAMP6. (ND – no detectable double label)

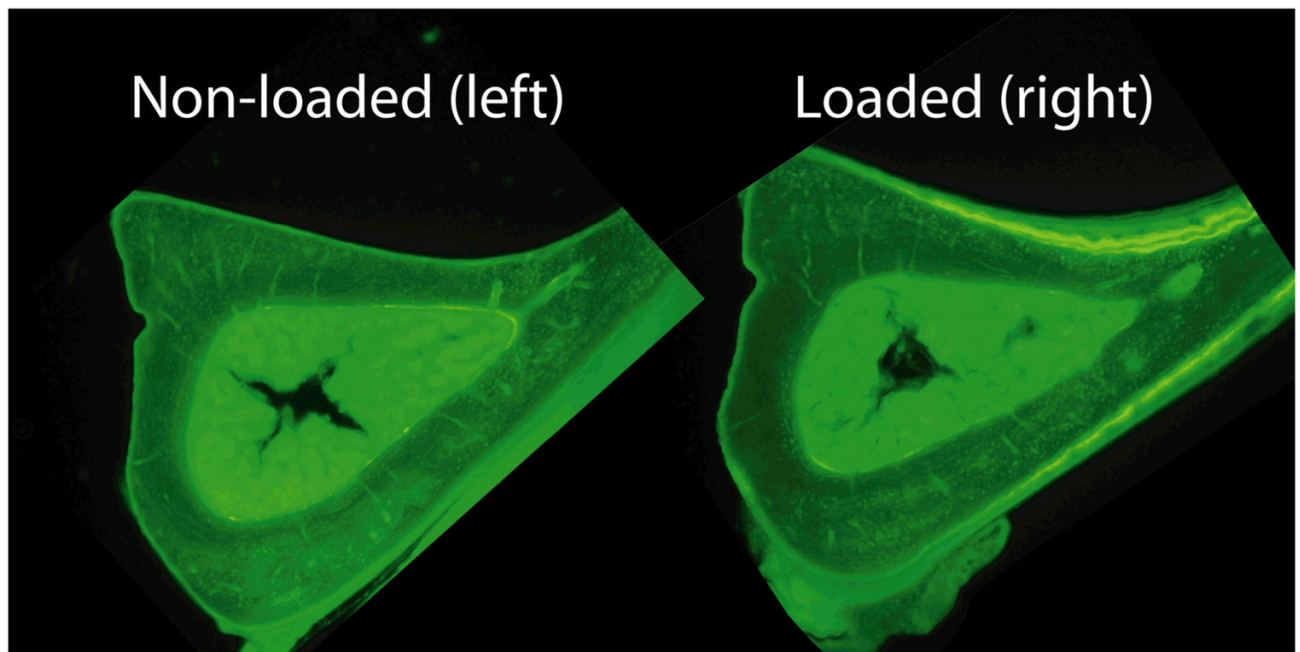


Figure 4. Fluorescent photomicrographs illustrating lack of endocortical bone response in tibia subjected to sham bending (right). (Sections shown are from a SAMR1 mouse subjected to high force 15.1 N periosteal compression.) Periosteal bone formation was activated, but in the absence of bending there was no detectable endocortical response.

Table 1

Compressive forces for in vivo tibial bending to produce estimated peak values of 1000 and 2000 $\mu\epsilon$ on endocortical surface of the tibial diaphysis in SAMR1 and SAMP6 mice [28].

Peak Endocortical Strain ($\mu\epsilon$)	SAMR1 (control)	SAMP6
1000	8.2 N	10.0 N
2000	15.1 N	17.7 N

Table 2

Endocortical bone formation indices (mean ± SD) from mice subjected to tibial bending. (n = 10–11 mice per group except as noted; 2–3 replicate sections per bone)

	SAMR1			SAMR1			SAMP6			SAMP6		
	1000 µε			2000 µε			1000 µε			2000 µε		
	Left	Right	R-L	Left	Right	R-L	Left	Right	R-L	Left	Right	R-L
	19.4 ± 14.5	28.0 ± 12.6	8.6 ± 17.5	17.7 ± 14.5	28.8 ± 16.0	10.8 ± 24.6	22.8 ± 11.1	35.5* ± 9.3	13.9* ± 13.1	32.1 ^{††} ± 6.8	33.0 ± 12.7	0.9 ^{††} ± 13.4
	0.0 ± 0.0	10.3* ± 14.3	10.3* ± 14.3	0.2 ± 0.5	32.5 ^{**††} ± 27.8	33.1 ^{**††} ± 27.6	0.1 ± 0.3	16.5* ± 12.2	16.4* ± 12.2	0.6 ± 1.8	16.0* ± 20.1	15.0* ± 20.7
	9.6 ± 7.4	24.3* ± 17.7	14.6* ± 15.8	8.9 ± 7.1	44.4 ^{**††} ± 22.1	38.5 ^{**††} ± 24.1	10.5 ± 5.0	34.3* ± 11.1	23.4* ± 9.9	16.6 ^{††} ± 3.0	32.1* ± 19.6	15.5* ± 21.3
	ND	20.2 ± 0.52 (n = 6)	NC	1.80 (n = 1)	2.85 ^{††} ± 1.11 (n = 9)	NC	1.57 (n = 1)	2.02 ± 0.66 (n = 9)	0.75 (n = 1)	1.36 (n = 2)	2.82 ^{††} ± 0.53 (n = 6)	1.2 (n = 1)
	ND	0.62 ± 0.45 (n = 6)	NC	0.06 (n = 1)	1.57 [†] ± 1.08 (n = 9)	NC	0.17 (n = 1)	0.75 ± 0.40 (n = 9)	0.79 (n = 1)	0.22 (n = 2)	1.25 [†] ± 0.56 (n = 6)	0.35 (n = 1)

Left (non-loaded), paired t-test

1000 µε group of same mouse strain, ANOVA

†; NC = cannot compute because there are no pairs with data for both left and right Due to the low incidence of double labels in non-loaded (left) tibiae, statistical between loaded and non-loaded bones could not be performed.

Endocortical bone formation indices (mean \pm SD) from mice subjected to **sham** tibial bending. "All subgroups" is based on fourteen mice (two SAMR1 loaded at 8.2 N; eight SAMR1 at 15.1 N; two SAMP6 at 10 N; two SAMP6 at 17.7 N). (2–3 replicate sections analyzed per bone)

Table 3

Outcome	All subgroups (n = 14)			SAMR1/15.1 N (n = 8)		
	Left	Right	R-L	Left	Right	R-L
sLS/BS (%)	21.8 \pm 14.3	21.4 \pm 12.0	-0.5 \pm 11.7	20.4 \pm 11.7	16.6 \pm 11.2	-3.8 \pm 12.1
dLS/BS (%)	0.2 \pm 0.6	1.6 \pm 4.4	1.5 \pm 4.5	0.3 \pm 0.8	0.0 \pm 0.0	-0.3 \pm 0.8
MS/BS (%)	11.1 \pm 7.4	12.3 \pm 9.3	1.2 \pm 6.4	10.5 \pm 6.4	8.3 \pm 5.6	-2.2 \pm 6.3
MAR ($\mu\text{m}/\text{day}$)	0.93 (n = 1)	1.19 (n = 2)	NC	0.93 (n = 1)	ND	NC
BFR/BS ($\mu\text{m}^3/\mu\text{m}^3/\text{day}$)	0.30 (n = 1)	0.40 (n = 2)	NC	0.30 (n = 1)	ND	NC

ND = no detectable double label; NC = cannot compute because there are no pairs with data for both left and right

Percent positively stained area from cultures of bone marrow taken from tibiae subjected to bending (right) and control (left). Wells were stained for alkaline phosphatase (ALP, day 14) or alizarin red (ALIZ, day 28). Values are the mean \pm SD based on 6–10 tibia per group, with 2–4 replicate wells per bone.

Table 4

Mouse Strain	Mechanical Strain	ALP		ALP		ALIZ	
		Left (control)	Right (loaded)	Left (control)	Right (loaded)	Left (control)	Right (loaded)
SAMR1 (control)	1000 $\mu\epsilon$	9.0 \pm 5.5	12.3 \pm 6.4	4.8 \pm 3.7	4.0 \pm 2.6		
	2000 $\mu\epsilon$	10.8 \pm 7.2	9.8 \pm 7.0	2.3 \pm 1.7	2.5 \pm 2.2		
SAMP6	1000 $\mu\epsilon$	13.7 \pm 13.9	12.1 \pm 14.8	15.7 \pm 18.0	11.7 \pm 16.5		
	2000 $\mu\epsilon$	7.5 \pm 7.2	9.0 \pm 10.8	16.8 \pm 14.7	12.2 \pm 13.1		